mathematics

MDPI

Article

A Statistical Reliability Framework for Markov Epidemic Networks

M. A. Sohaly *, M. F. Al-Harbi, M. M. Al-Buhairi, K. A. Alwshmi, N. A. Alqussyer and T. M. Alnoushan

Department of Statistics and Operations Research, College of Science, Qassim University, Buraydah 51452, Saudi Arabia; 422214708@qu.edu.sa or wwwfofo.al@gmail.com (M.F.A.-H.); 421203401@qu.edu.sa or mashaelmohalb@outlook.com (M.M.A.-B.); 443200986@qu.edu.sa or kadiali0833@gmail.com (K.A.A.); 432214530@qu.edu.sa or najlaalqussyer@gmail.com (N.A.A.); 432204575@qu.edu.sa or talaalnoushan@gmail.com (T.M.A.)

* Correspondence: moh.elsayed@qu.edu.sa

Abstract

Disease progression can be statistically represented as a network of patient states connected by transition probabilities, providing a natural basis for quantifying progression toward favorable and unfavorable outcomes. This study develops a statistical reliability framework for disease progression networks based on discrete-time Markov transitions, integrating maximum-likelihood estimation, first-passage reliability, bootstrap uncertainty quantification, and probability-simplex-constrained sensitivity analysis. The framework converts patient-level longitudinal trajectories into an estimated transition structure and subsequently quantifies the probability of reaching a favorable target state before an absorbing unfavorable outcome. A row-preserving perturbation strategy is used to assess the influence of individual transitions while maintaining the probability constraints, and a dimensionless elasticity measure is introduced to rank transitions according to their contribution to network reliability. Monte Carlo experiments demonstrate stable statistical performance of the proposed estimator: for the specified baseline network, the true reliability is approximately 0.7483, while the RMSE decreases from 0.0465 for $n = 100$ to 0.0098 for $n = 2000$, indicating substantial improvement in estimation accuracy as the sample size increases. The sensitivity analysis further identifies the most influential transitions, with progression from localized disease to treatment and treatment to remission showing the strongest positive effects on reliability, whereas transitions toward death exhibit negative effects. The framework is also applied to a real longitudinal breast cancer dataset comprising 169 patient records. The empirical analysis identifies 16 recurrence events and four deaths and characterizes the observed treatment, surgery, recurrence, and survival-time patterns. Importantly, because the available clinical variables do not unambiguously identify all states of the theoretical seven-state model, the real-data analysis is restricted to directly observable patient events rather than imposing unsupported clinical state assignments. Overall, the results demonstrate that the proposed framework provides a statistically interpretable pipeline linking patient-level transition data, network reliability, uncertainty quantification, and transition importance, with potential applications to reliability-based analysis of multistate disease progression and other longitudinal health processes.

Keywords: epidemic; discrete-time Markov chain; network reliability; mathematical model; bootstrap; simulation; breast cancer

MSC: 60J10; 90B25; 62P10

Check for updates

Academic Editors: Wei Yao and Hongying Shu

Received: 14 September 2026
Revised: 16 October 2026
Accepted: 20 October 2026
Published: 26 October 2026

Copyright: © 2026 by the authors. Licensee MDPI, Basel, Switzerland. This article is an open access article distributed under the terms and conditions of the Creative Commons Attribution (CC BY) license.

1. Introduction

Disease progression is often observed longitudinally through a sequence of clinically meaningful patient states. A patient may move from an initial state to early detection, localized disease, treatment, remission, metastasis, or death. Such progression can naturally be represented by a directed graph in which vertices correspond to patient states and directed edges represent possible transitions between consecutive observations—see [1,2].

1.1. Literature Review

Multistate Markov models provide a well-established statistical framework for describing disease progression and estimating transition behavior from longitudinal observations [3,4]. These models have been applied to a wide range of medical processes in which patients move among clinically defined states. Recent methodological developments continue to emphasize the flexibility of multistate models for analyzing complex state-transition processes [5]. Zingoni et al. [6] reviewed multistate modelling approaches for monitoring disease progression, including Bayesian estimation based on the Kolmogorov–Chapman forward equations. More recently, Akwiwu et al. [7] compared methods for modelling multistate cancer progression using screening data with censoring after intervention. In discrete-time settings, transition probabilities can be estimated directly from observed patient trajectories, and the resulting transition matrix provides a natural basis for statistical analysis of functions of the transition process [8,9]. At the same time, assumptions concerning the Markov property, state definition, and model specification can substantially affect inference and therefore require appropriate assessment [10].

Beyond the formulation of multistate models, previous studies have examined the statistical challenges arising when transition processes are inferred from longitudinal clinical data. Jackson et al. [3] considered multistate Markov models for disease progression in the presence of classification error, highlighting the importance of distinguishing the underlying clinical states from their observed classifications. Titman and Sharples [10] investigated diagnostic methods for multistate models, emphasizing the need to assess model adequacy when drawing statistical conclusions from estimated transition structures. In addition, Welton and Ades [9] studied the estimation of Markov transition probabilities and rates from fully and partially observed data, with particular attention to uncertainty propagation and model calibration. These studies establish important foundations for statistical inference in multistate systems. However, when the scientific objective is to quantify the probability of reaching a specified target state before an adverse absorbing state, the uncertainty in the estimated transition structure must be related to the resulting first-passage probability. This motivates the outcome-oriented reliability analysis developed in the present study.

Multistate reliability theory extends the classical binary reliability setting by allowing system and component performance to be represented through multiple states and by relating state configurations to system-level performance measures [11]. Beyond clinical applications, Tanchev et al. [2] developed a Bayesian graph-based Markov chain model for African swine fever transmission, illustrating the use of network-based Markov models in epidemic transmission analysis. This perspective provides a natural connection with disease-progression networks, where patients occupy multiple clinical states and the overall outcome depends on the sequence of transitions among these states. In the present setting, this reliability perspective is formulated through the probability of reaching a desirable clinical state before entering an absorbing adverse state, thereby connecting multistate disease progression with first-passage reliability.

1.2. Novelty and Contribution

Although multistate Markov models provide a natural description of disease progression, the estimated transition matrix itself does not directly provide a reliability measure for an outcome-oriented clinical question. In particular, when remission is viewed as a desirable target and death as an adverse absorbing state, it is useful to quantify the probability that a patient reaches remission before death. This motivates a reliability interpretation of the disease progression network. The resulting reliability is a nonlinear function of the estimated transition probabilities, so uncertainty in transition estimation must also be propagated to the reliability measure.

The present study does not claim novelty for the individual statistical components, which are established in the literature. Instead, its methodological contribution lies in their integration into a single statistical workflow. Specifically, the framework connects (i) transition-probability estimation from longitudinal patient trajectories, (ii) first-hit network reliability, (iii) patient-level bootstrap uncertainty quantification, and (iv) probability-constrained sensitivity analysis of individual transitions. This integration provides a direct pathway from observed patient trajectories to an outcome-oriented reliability measure and then to transition-level importance, while preserving the stochastic constraints of the transition matrix. A related network-level perspective is also emphasized in recent resilience modeling of engineered networks under recurrent hazards, where overall system performance is determined by the collective evolution of multiple performance states and their transitions [12]. Although that setting concerns engineered systems rather than disease progression, the underlying network-level perspective is relevant here: individual transitions contribute jointly to an overall system-level performance measure. In the present framework, this role is played by the first-passage reliability $\mathcal{R}_H$, which aggregates the admissible disease-progression pathways into a single outcome-oriented measure. Thus, the framework links estimation, reliability, uncertainty assessment, and transition interpretation within one statistically coherent procedure.

$$\boxed{\text{patient trajectories} \longrightarrow \widehat{P} \longrightarrow \widehat{\mathcal{R}}_H \longrightarrow CI_{95\%} \longrightarrow \text{transition importance.}}$$

The main research question is as follows:

> Which transitions in a disease progression network have the greatest statistical influence on the probability of reaching remission before death?

A related question is how uncertainty in the estimated transition probabilities affects the resulting disease-network reliability. These questions motivate the use of patient-level bootstrap resampling and a row-preserving sensitivity analysis that respects the stochastic constraints of the transition matrix.

The framework is formulated at the patient level, with clinical states represented as vertices and observed transitions represented as directed edges. It therefore provides a statistical representation of clinical progression rather than a mechanistic model of disease biology. The methodology is illustrated in a breast-cancer progression setting and evaluated through a Monte Carlo simulation study.

2. Graph-Based Markov Disease Progression Model

Let

$$G = (V, E)$$

be a directed disease progression graph, where V is the set of clinically defined patient states and E is the set of admissible transitions between states. For the illustrative breast-cancer setting, consider the state space $V = H, E, L, T, R, M, D$, as in Table 1.

Table 1. Definition of the disease progression states.

State	Description
H	Initial (healthy) state
E	Early detection
L	Localized cancer
T	Treatment
R	Remission
M	Distant metastasis
D	Death

The admissible inter-state transitions are in Figure 1.

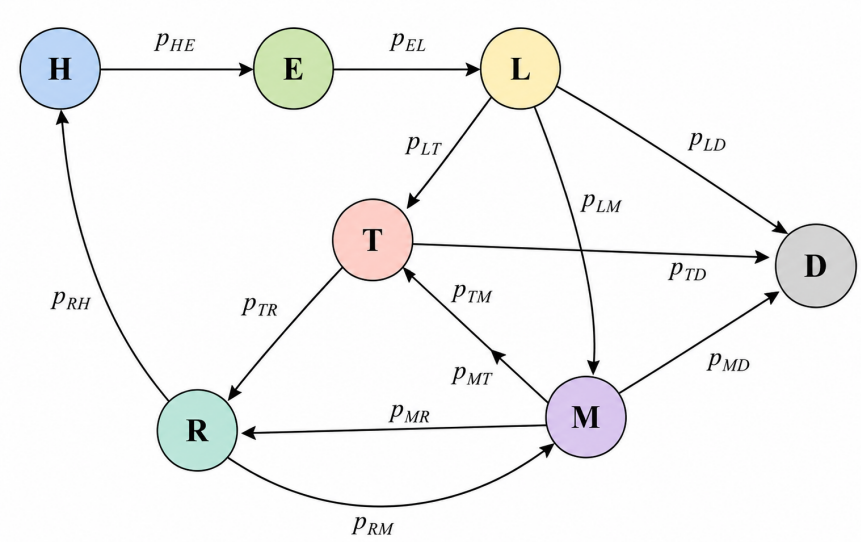


Figure 1. Patient-level disease progression network. Nodes represent clinically defined patient states, while directed edges represent possible transitions between distinct states. Self-transitions are represented in the transition matrix and omitted from the graph for visual clarity.

The state D is absorbing. Self-transitions are also allowed and are represented by the diagonal elements of the transition matrix. For visual clarity, these self-transitions are omitted from the network diagram. The graph is defined at the patient level: each vertex represents a clinically defined state of a patient, while each directed edge represents a possible transition between two consecutive observation occasions. Thus, the graph describes the statistical structure of patient-level disease progression rather than a mechanistic interaction among individual cancer cells.

Discrete-Time Markov Assumption

Let X_t denote the clinical state of a patient at observation occasion t. The index t represents successive observation occasions on a common discrete time scale. We assume a first-order Markov property:

$$P(X_{t+1} = j \mid X_t = i, X_{t-1}, \ldots, X_0) = P(X_{t+1} = j \mid X_t = i).$$

For $i, j \in V$, define the one-step transition probability by

$$p_{ij} = P(X_{t+1} = j \mid X_t = i).$$

In practical applications, the discrete observation cycle should be selected according to the clinical follow-up schedule and the temporal resolution at which clinically meaningful

state changes can be distinguished. When observation times are irregular, the recorded times should first be mapped to a clinically meaningful common observation scale before one-step transition probabilities are estimated. The chosen cycle should be sufficiently short to represent relevant changes in disease status, while avoiding unnecessary sparsity in the transition counts. If transition times remain substantially heterogeneous or the timing of transitions is itself of primary interest, a continuous-time multistate model may be more appropriate. The transition matrix is

$$P = (p_{ij})_{i,j \in V},$$

where

$$p_{ij} \geq 0, \qquad \sum_{j \in V} p_{ij} = 1 \quad \text{for every } i \in V.$$

Using the state ordering

$$(H, E, L, T, R, M, D),$$

the transition matrix takes the form

$$P = \begin{pmatrix} p_{HH} & p_{HE} & 0 & 0 & 0 & 0 & 0 \\ 0 & p_{EE} & p_{EL} & 0 & 0 & 0 & 0 \\ 0 & 0 & p_{LL} & p_{LT} & 0 & p_{LM} & p_{LD} \\ 0 & 0 & 0 & p_{TT} & p_{TR} & p_{TM} & p_{TD} \\ p_{RH} & 0 & 0 & 0 & p_{RR} & p_{RM} & 0 \\ 0 & 0 & 0 & p_{MT} & p_{MR} & p_{MM} & p_{MD} \\ 0 & 0 & 0 & 0 & 0 & 0 & 1 \end{pmatrix}.$$

The Markov property is a modeling assumption and should be assessed when longitudinal data are available. Patient heterogeneity, unequal observation intervals, state misclassification, or dependence on a longer history may require an extended multistate formulation [3,5,10]. Figure 2 illustrates the discrete-time Markov assumption for disease progression.

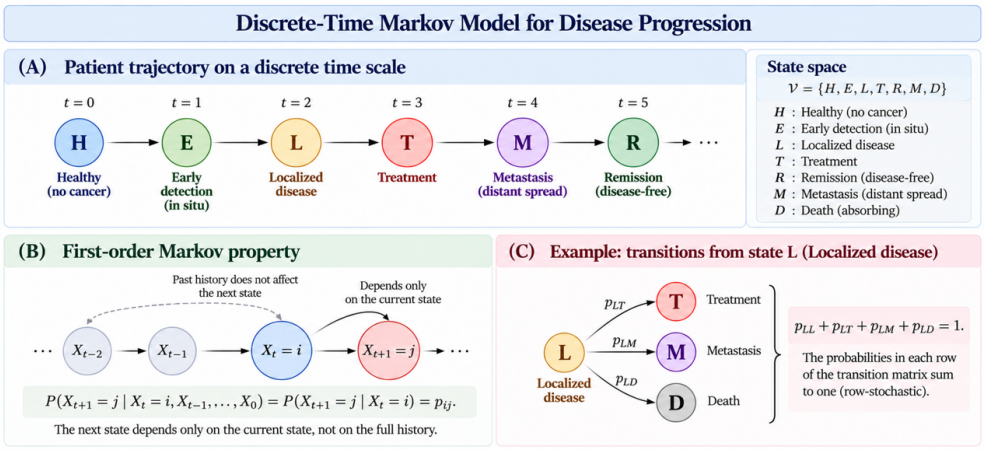


Figure 2. Illustration of the discrete-time Markov assumption for disease progression. The figure shows an example patient trajectory, the first-order Markov property, and the conditional distribution of the next state given the current state.

3. Disease-Network Reliability

The directed disease progression network defines several possible pathways through which a patient may move from the initial state toward either a desirable or an adverse

outcome. To obtain an outcome-oriented measure of the network, we define reliability in terms of the first arrival at remission before death.

Let

$$\tau_R = \inf\{t \geq 0 : X_t = R\}$$

denote the first observation occasion at which the patient enters the remission state, and let

$$\tau_D = \inf\{t \geq 0 : X_t = D\}$$

denote the first observation occasion at which the patient enters the death state. For an initial state $i \in V$, define the disease-network reliability by

$$\mathcal{R}_i = P_i(\tau_R < \tau_D).$$

The primary reliability measure considered in this study is therefore

$$\boxed{\mathcal{R}_H = P_H(\tau_R < \tau_D).}$$

Thus, $\mathcal{R}_H$ represents the probability that a patient starting from the initial state H reaches remission before death. This definition is a first-hit reliability measure. In particular, once the process reaches R for the first time, the event $\{\tau_R < \tau_D\}$ has occurred. Consequently, subsequent transitions from R do not affect the value of $\mathcal{R}_H$. This distinction is important because remission is not required to be a permanent clinical state for the proposed reliability measure.

3.1. First-Step Reliability Equations

Let the transient states with respect to the reliability event be

$$\mathcal{T} = \{H, E, L, T, M\},$$

while the target and failure states are

$$\mathcal{A} = \{R, D\}.$$

For each transient state $i \in \mathcal{T}$, define

$$r_i = P_i(\tau_R < \tau_D).$$

The boundary conditions are

$$r_R = 1, \qquad r_D = 0.$$

Applying the law of total probability after one transition gives

$$r_i = \sum_{j \in \mathcal{T}} p_{ij} r_j + p_{iR}, \qquad i \in \mathcal{T}.$$

The term p_{iD} does not appear explicitly because a transition to D contributes zero to the probability of reaching R before D. Let

$$Q = (p_{ij})_{i,j \in \mathcal{T}}$$

denote the transient-to-transient transition matrix and define

$$\mathbf{b} = \begin{pmatrix} p_{HR} \\ p_{ER} \\ p_{LR} \\ p_{TR} \\ p_{MR} \end{pmatrix}.$$

For the specific network considered here,

$$p_{HR} = p_{ER} = p_{LR} = 0,$$

and hence

$$\mathbf{b} = \begin{pmatrix} 0 \\ 0 \\ 0 \\ p_{TR} \\ p_{MR} \end{pmatrix}.$$

Writing

$$\mathbf{r} = \begin{pmatrix} r_H \\ r_E \\ r_L \\ r_T \\ r_M \end{pmatrix},$$

The first-step equations can be written compactly as

$$\mathbf{r} = \mathbf{Q}\mathbf{r} + \mathbf{b}.$$

Therefore,

$$(\mathbf{I} - \mathbf{Q})\mathbf{r} = \mathbf{b},$$

and, provided that the transient subnetwork is proper,

$$\boxed{\mathbf{r} = (\mathbf{I} - \mathbf{Q})^{-1}\mathbf{b}.}$$

Consequently, the reliability for a patient starting in H is

$$\boxed{\mathcal{R}_H = \mathbf{e}_H^\top (\mathbf{I} - \mathbf{Q})^{-1}\mathbf{b}} \tag{1}$$

where

$$\mathbf{e}_H = (1, 0, 0, 0, 0)^\top.$$

The matrix

$$\mathbf{N} = (\mathbf{I} - \mathbf{Q})^{-1}$$

is the fundamental matrix of the transient part of the absorbing Markov chain [13]. Its use here provides a direct connection between the estimated transition structure and the probability of reaching the desired outcome before failure. For the specific disease-progression network considered here, the first-step equations can also be written explicitly as follows:

$$r_H = p_{HH} r_H + p_{HE} r_E,$$

$$r_E = p_{EE} r_E + p_{EL} r_L,$$

$$r_L = p_{LL} r_L + p_{LT} r_T + p_{LM} r_M,$$

$$r_T = p_{TT} r_T + p_{TR} + p_{TM} r_M,$$

and

$$r_M = p_{MT} r_T + p_{MR} + p_{MM} r_M.$$

Because the rows corresponding to H and E contain only a self-loop and one forward transition, their eventual reliability is unchanged by the waiting probability. Hence,

$$r_H = r_E = r_L.$$

Define

$$\Delta = (1 - p_{TT})(1 - p_{MM}) - p_{TM} p_{MT}.$$

Provided that $\Delta > 0$, the reliability probabilities associated with the treatment and metastasis states are

$$\boxed{r_T = \frac{p_{TR}(1 - p_{MM}) + p_{TM} p_{MR}}{\Delta}}$$

and

$$\boxed{r_M = \frac{(1 - p_{TT}) p_{MR} + p_{MT} p_{TR}}{\Delta}.}$$

Consequently, the reliability from the localized-disease state is

$$\boxed{r_L = \frac{p_{LT} r_T + p_{LM} r_M}{1 - p_{LL}}}$$

and, since $r_H = r_E = r_L$,

$$\boxed{\mathcal{R}_H = r_H = r_E = r_L.}$$

These expressions provide an explicit interpretation of the reliability measure in terms of the transition probabilities. In particular, transitions into remission, transitions toward metastasis, and transitions from metastasis back to treatment or remission jointly determine the probability of reaching remission before death.

3.2. Interpretation

The quantity $\mathcal{R}_H$ summarizes the probability of reaching remission before death over all admissible disease-progression pathways starting from the initial state H. In matrix form, see Equation (1), where $(\mathbf{I} - \mathbf{Q})^{-1}$ accounts for repeated visits to transient states and $\mathbf{b}$ represents the one-step transitions into the remission state. Thus, $\mathcal{R}_H$ is a network-level probability rather than a single transition probability such as p_{TR} or p_{MR}.

The matrix formulation automatically combines alternative pathways and their associated transition probabilities. Consequently, changes in one transition probability may affect $\mathcal{R}_H$ indirectly through subsequent transitions and repeated movements among transient states.

The reliability measure is also distinct from the probability of remaining in remission after treatment. The present analysis concerns only the ordering of the first occurrence of remission and death,

$$\tau_R < \tau_D.$$

Thus, once remission is reached for the first time, the reliability event has occurred, regardless of subsequent transitions from the remission state. This first-hit formulation allows the proposed measure to be used for comparing estimated disease-transition networks

and for quantifying how statistical uncertainty or admissible perturbations in individual transition probabilities influence the overall probability of successful progression.

4. Statistical Estimation of Transition Probabilities

Suppose that longitudinal patient records are observed at successive observation occasions on a common discrete time scale. For each pair of states (i, j), let

$$n_{ij} = \#\{\text{observed transitions from state } i \text{ to state } j\}$$

denote the number of observed transitions from state i to state j. The total number of observed transitions originating from state i is

$$n_i = \sum_{j \in V} n_{ij}.$$

For a fully observed discrete-time Markov chain, the transition counts within each row of the transition matrix follow a multinomial structure. Consequently, the likelihood of the transition matrix, up to a multiplicative constant that does not depend on P, is

$$L(P) \propto \prod_{i \in V} \prod_{j \in V} p_{ij}^{n_{ij}},$$

subject to the stochastic constraints

$$p_{ij} \geq 0, \qquad \sum_{j \in V} p_{ij} = 1, \qquad i \in V.$$

Maximizing the likelihood under these constraints gives the maximum-likelihood estimator

$$\boxed{\widehat{p}_{ij} = \frac{n_{ij}}{n_i}, \qquad n_i > 0.}$$

Thus, each estimated transition probability is the observed proportion of transitions from state i that subsequently enter state j. This estimator is the standard maximum-likelihood estimator for a fully observed discrete-time Markov transition matrix [8,9]. Transitions that are not allowed by the disease progression graph are treated as structural zeros. Therefore,

$$\widehat{p}_{ij} = 0$$

for any transition $i \to j$ that is excluded from the proposed network.

The diagonal elements $\widehat{p}_{ii}$ represent the probability that a patient remains in the same state between two consecutive observation occasions. These self-transitions are retained in the transition matrix because they are part of the Markov representation, even though they are omitted from the graphical visualization for clarity.

5. Estimated Disease-Network Reliability

After estimating the transition matrix $\hat{P}$, the corresponding transient-to-transient submatrix is obtained as

$$\hat{Q} = \hat{P}_{\mathcal{T},\mathcal{T}},$$

where

$$\mathcal{T} = \{H, E, L, T, M\}.$$

For the proposed disease-progression network, the vector of estimated one-step transitions directly into remission is

$$\hat{\mathbf{b}} = \begin{pmatrix} 0 \\ 0 \\ 0 \\ \hat{p}_{TR} \\ \hat{p}_{MR} \end{pmatrix}.$$

The estimated vector of first-hit remission probabilities is therefore

$$\boxed{\hat{\mathbf{r}} = (I - \hat{Q})^{-1}\hat{\mathbf{b}},}$$

provided that the estimated transient subnetwork is proper. The estimated reliability for a patient initially in state H is consequently

$$\boxed{\hat{\mathcal{R}}_H = \mathbf{e}_H^{\top}(I - \hat{Q})^{-1}\hat{\mathbf{b}}.}$$

Thus, the proposed estimator is obtained by substituting the statistically estimated transition probabilities into the first-step reliability formulation. It incorporates all admissible pathways from the initial state to remission and automatically accounts for competing transitions to death.

Importantly, $\hat{\mathcal{R}}_H$ is a nonlinear function of the estimated transition probabilities. Therefore, uncertainty in $\hat{P}$ propagates through $(I - \hat{Q})^{-1}$ and affects the resulting reliability estimate. This motivates the bootstrap procedure developed in the next section.

Statistical Interpretation

The estimation procedure separates the analysis into two stages. First, the transition probabilities are estimated directly from the observed patient trajectories. Second, the estimated transition matrix is transformed into the disease-network reliability measure. Thus, the overall estimation pipeline can be summarized as

$$\text{Observed transitions} \longrightarrow \hat{P} \longrightarrow (\hat{Q}, \hat{\mathbf{b}}) \longrightarrow \hat{\mathcal{R}}_H.$$

This separation is useful because uncertainty in the observed transition counts is subsequently propagated to the reliability estimate through the bootstrap procedure presented in Section 5.

The direct count estimator assumes that the relevant states and transitions are observed without ambiguity at the specified observation occasions. In practice, patient records may contain missing visits, unequal observation intervals, misclassification of disease states, or unobserved intermediate transitions. Under such circumstances, the simple empirical estimator may no longer be sufficient, and more general multistate estimation procedures may be required [3,4]. These issues are treated as extensions and limitations of the present discrete-time framework rather than as additional modeling assumptions.

For practical applications, the discrete-time cycle length should be selected according to the clinical follow-up schedule and the time scale over which a transition can reasonably be regarded as occurring within one observation interval. A common cycle length should then be used when successive observations are treated as Markov transitions. If the recorded follow-up times are substantially irregular, the observations should not automatically be interpreted as transitions on an identical time scale. Instead, the records may be organized into prespecified observation windows when clinically appropriate. When the timing of transitions itself is of primary interest or a common observation scale cannot be justified, continuous-time or other general multistate methods may be more appropriate.

6. Bootstrap Uncertainty Quantification

The estimated disease-network reliability is a nonlinear function of the estimated transition probabilities. Consequently, sampling uncertainty in $\hat{P}$ propagates through the fundamental-matrix calculation and affects the resulting estimate $\hat{\mathcal{R}}_H$. To quantify this uncertainty without relying on a closed-form variance expression, a patient-level nonparametric bootstrap procedure is employed.

Let B denote the number of bootstrap replications. For each replication $b = 1, \ldots, B$, a bootstrap sample is generated by resampling complete patient trajectories with replacement from the original sample. If the original dataset contains n patients, each bootstrap sample therefore contains n complete trajectories. The transition counts are recalculated from the resampled trajectories, giving

$$n_{ij}^{*(b)} = \#\{\text{resampled transitions } i \to j\},$$

and the corresponding transition probabilities are estimated by

$$\hat{p}_{ij}^{*(b)} = \frac{n_{ij}^{*(b)}}{n_i^{*(b)}}, \qquad n_i^{*(b)} > 0.$$

The bootstrap transient matrix and remission-entry vector are then constructed as

$$\hat{Q}^{*(b)} = \hat{P}_{\mathcal{T},\mathcal{T}}^{*(b)}$$

and

$$\hat{\mathbf{b}}^{*(b)} = \begin{pmatrix} 0 \\ 0 \\ 0 \\ \hat{p}_{TR}^{*(b)} \\ \hat{p}_{MR}^{*(b)} \end{pmatrix}.$$

The reliability is subsequently recalculated for each bootstrap sample according to

$$\boxed{\widehat{\mathcal{R}}_H^{*(b)} = \mathbf{e}_H^\top \left(I - \widehat{Q}^{*(b)} \right)^{-1} \widehat{\mathbf{b}}^{*(b)}} \tag{2}$$

The resulting values

$$\hat{\mathcal{R}}_H^{*(1)}, \ldots, \hat{\mathcal{R}}_H^{*(B)}$$

form the empirical bootstrap distribution of the estimated disease-network reliability. A percentile-based 95% bootstrap confidence interval is then obtained from the empirical quantiles of this distribution as

$$\boxed{CI_{95\%} = \left[\widehat{\mathcal{R}}_{H,(0.025)}^{*}, \widehat{\mathcal{R}}_{H,(0.975)}^{*} \right]} \tag{3}$$

Thus, the bootstrap procedure propagates patient-level sampling variability from the observed transition histories through the estimated transition matrix and ultimately to the disease-network reliability.

Interpretation of Bootstrap Uncertainty

The bootstrap distribution provides an empirical assessment of the sampling variability of $\widehat{\mathcal{R}}_H$. A narrow confidence interval indicates relatively stable estimation of the

reliability, whereas a wider interval indicates greater statistical uncertainty in the estimated disease-network reliability.

Importantly, the confidence interval quantifies uncertainty for the reliability estimate obtained from the observed sample. It should not be interpreted as an empirical coverage probability. Evaluation of the actual coverage probability of the proposed confidence interval requires repeated independent datasets generated under a specified data-generating mechanism, which is addressed separately in the Monte Carlo simulation study.

The bootstrap approach is particularly useful here because the reliability measure is a nonlinear function of several estimated transition probabilities. It therefore avoids the need to derive a closed-form sampling variance for

$$\boxed{\widehat{\mathcal{R}}_H = \mathbf{e}_H^\top (I - \widehat{Q})^{-1} \widehat{\mathbf{b}}} \tag{4}$$

Bootstrap-based uncertainty assessment for functions of estimated discrete-time Markov transition matrices has been considered in the statistical literature [8], while the general theoretical foundation of the nonparametric bootstrap is given by Efron and Tibshirani [14].

7. Constrained Reliability Sensitivity Analysis

Because every row of a transition matrix is required to satisfy

$$\sum_{j \in V} p_{ij} = 1,$$

transition probabilities cannot generally be perturbed independently. A sensitivity analysis must therefore preserve the stochastic structure of the transition matrix. For a selected admissible transition $i \to j$, consider first a positive perturbation

$$p_{ij}^{+} = p_{ij} + \delta,$$

where $\delta > 0$ is sufficiently small. The remaining nonzero outgoing probabilities in row i are rescaled proportionally according to

$$p_{ik}^{+} = p_{ik} \frac{1 - p_{ij} - \delta}{1 - p_{ij}}, \qquad k \neq j.$$

For a negative perturbation, define

$$p_{ij}^{-} = p_{ij} - \delta,$$

with the remaining nonzero outgoing probabilities given by

$$p_{ik}^{-} = p_{ik} \frac{1 - p_{ij} + \delta}{1 - p_{ij}}, \qquad k \neq j.$$

In the numerical sensitivity analysis, the baseline perturbation size is set to $\delta = 0.005$. To assess the numerical stability of the resulting elasticity ranking, additional calculations are performed using $\delta = 0.001$ and $\delta = 0.01$. In all cases, the perturbed transition probabilities remain within $[0, 1]$, and the row-sum constraint is preserved. Under these constructions, the stochastic row constraint is preserved. Indeed,

$$\sum_{k} p_{ik}^{+} = p_{ij} + \delta + (1 - p_{ij}) \frac{1 - p_{ij} - \delta}{1 - p_{ij}} = 1,$$

and similarly,

$$\sum_k p_{ik}^- = p_{ij} - \delta + (1 - p_{ij})\frac{1 - p_{ij} + \delta}{1 - p_{ij}} = 1.$$

Let P^+ and P^- denote the transition matrices obtained from these row-preserving perturbations. The corresponding reliabilities are

$$\mathcal{R}_H(P^+) = \mathbf{e}_H^\top (\mathbf{I} - \mathbf{Q}^+)^{-1}\mathbf{b}^+,$$

and

$$\mathcal{R}_H(P^-) = \mathbf{e}_H^\top (\mathbf{I} - \mathbf{Q}^-)^{-1}\mathbf{b}^-.$$

The numerical local sensitivity of the reliability with respect to the selected transition is estimated by the central finite difference

$$\boxed{S_{ij} = \frac{\mathcal{R}_H(P^+) - \mathcal{R}_H(P^-)}{2\delta}.}$$

This measure quantifies the local change in disease-network reliability resulting from a small admissible perturbation of the selected transition probability while maintaining the normalization of its transition row. To facilitate comparisons across transitions with different baseline probabilities, a scale-free elasticity measure is defined as

$$\boxed{E_{ij} = \frac{p_{ij}}{\mathcal{R}_H} S_{ij}.}$$

Thus, E_{ij} represents the approximate proportional change in $\mathcal{R}_H$ associated with a proportional change in p_{ij} under the specified row-preserving perturbation.

Positive values of E_{ij} indicate that increasing the selected transition tends to increase the probability of reaching remission before death. Negative values indicate that increasing the selected transition tends to reduce this probability. The magnitude $|E_{ij}|$ can therefore be used to rank transitions according to their local influence on the overall disease-network reliability.

Analytical Sensitivity Representation

The numerical sensitivity analysis can also be expressed analytically. Let

$$\mathbf{N} = (\mathbf{I} - \mathbf{Q})^{-1}$$

denote the fundamental matrix. Differentiating the identity

$$N(\mathbf{I} - \mathbf{Q}) = I$$

gives

$$dN = N(dQ)N.$$

Since

$$\mathbf{r} = N\mathbf{b},$$

its differential is

$$d\mathbf{r} = dN\,\mathbf{b} + N\,d\mathbf{b}.$$

Substituting $dN = N(dQ)N$ and using $\mathbf{r} = N\mathbf{b}$ gives

$$\boxed{d\mathbf{r} = N[(dQ)\mathbf{r} + d\mathbf{b}].}$$

Because

$$\mathcal{R}_H = \mathbf{e}_H^\top \mathbf{r},$$

the corresponding differential of the reliability is

$$\boxed{d\mathcal{R}_H = \mathbf{e}_H^\top N[(dQ)\mathbf{r} + d\mathbf{b}].}$$

This expression shows that the effect of a transition perturbation is determined not only by the transition itself, but also by its position within the entire disease progression network. A transition can therefore have a substantial effect on $\mathcal{R}_H$ even when its individual probability is not among the largest entries of the transition matrix. Figure 3 shows the local influence of admissible disease-state transitions on disease-network reliability.

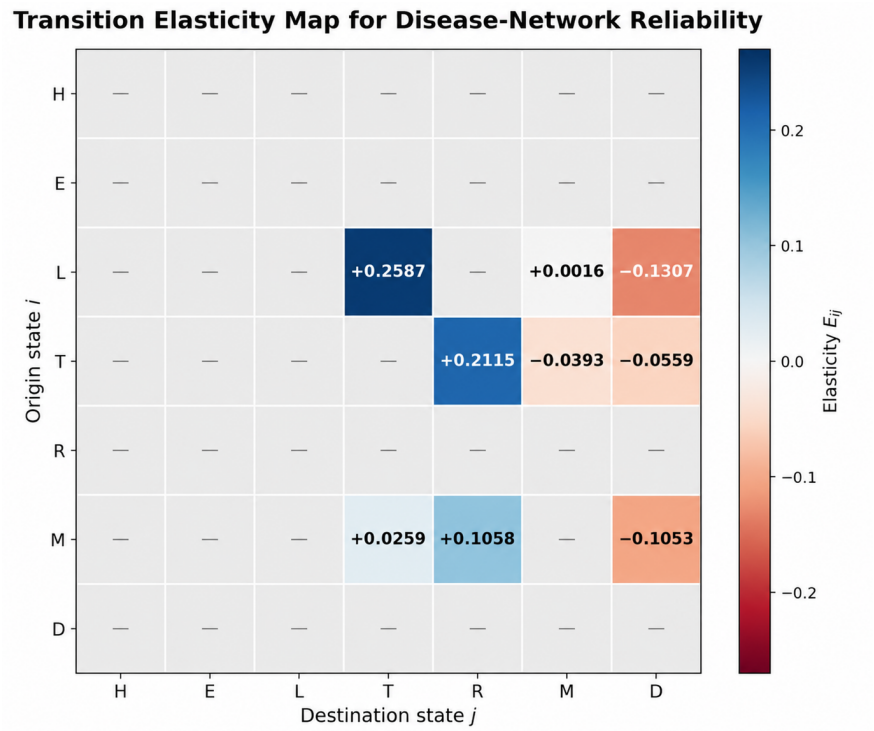


Figure 3. Transition elasticity map showing the local influence of admissible disease-state transitions on disease-network reliability. Positive values indicate transitions that increase reliability when perturbed upward, whereas negative values indicate transitions that decrease reliability.

The analytical expression provides the theoretical basis for the numerical sensitivity calculation and confirms that the sensitivity analysis must account for the dependence among transition probabilities within each stochastic row.

8. Monte Carlo Simulation Study

To evaluate the finite-sample performance of the proposed estimator, a controlled Monte Carlo simulation study is conducted using the following baseline transition matrix:

$$P_0 = \begin{pmatrix} 0.20 & 0.80 & 0 & 0 & 0 & 0 & 0 \\ 0 & 0.15 & 0.85 & 0 & 0 & 0 & 0 \\ 0 & 0 & 0.15 & 0.55 & 0 & 0.20 & 0.10 \\ 0 & 0 & 0 & 0.15 & 0.60 & 0.20 & 0.05 \\ 0.15 & 0 & 0 & 0 & 0.70 & 0.15 & 0 \\ 0 & 0 & 0 & 0.20 & 0.35 & 0.30 & 0.15 \\ 0 & 0 & 0 & 0 & 0 & 0 & 1 \end{pmatrix}.$$

The ordering of the states is

$$(H, E, L, T, R, M, D).$$

All rows of P_0 sum to one and all entries are nonnegative. The reliability corresponding to this baseline transition matrix is

$$\boxed{\mathcal{R}_H^{\text{true}} = \mathbf{e}_H^\top (\mathbf{I} - \mathbf{Q}_0)^{-1} \mathbf{b}_0 \approx 0.74828.}$$

This value is treated as the true reliability against which the Monte Carlo estimates are evaluated. A fixed random-number seed,

$$20260904,$$

is used to ensure reproducibility of the simulation experiment. Each simulated patient starts in the initial state H and follows the transition matrix until first reaching either remission R or death D. The resulting complete patient trajectory is then used to construct the transition counts required for estimation.

8.1. Simulation Design

The sample sizes considered are

$$n \in \{100, 250, 500, 1000, 2000\}.$$

For each sample size, $M = 300$ independent Monte Carlo datasets are generated. For each simulated dataset, the transition probabilities are estimated using

$$\widehat{p}_{ij} = \frac{n_{ij}}{n_i}, \qquad n_i > 0. \tag{5}$$

and using Equation (4), The finite-sample performance of the estimator is assessed using bias, root mean squared error (RMSE), empirical confidence-interval coverage, and average confidence-interval width.

$$\text{Bias} = \frac{1}{M} \sum_{m=1}^{M} \left(\widehat{\mathcal{R}}_H^{(m)} - \mathcal{R}_H^{\text{true}} \right),$$

and

$$RMSE = \sqrt{\frac{1}{M} \sum_{m=1}^{M} \left(\widehat{\mathcal{R}}_H^{(m)} - \mathcal{R}_H^{\text{true}} \right)^2}.$$

These measures quantify, respectively, the systematic deviation of the estimated reliability from its true value and the overall estimation error.

For each Monte Carlo replicate, a percentile bootstrap confidence interval with $B = 2000$ patient-level bootstrap replications is constructed. The empirical coverage probability is defined as

$$\widehat{\text{Coverage}} = \frac{1}{M} \sum_{m=1}^{M} I\left(\mathcal{R}_H^{\text{true}} \in CI_m \right),$$

where CI_m denotes the 95% percentile bootstrap confidence interval from the mth simulated dataset. The average confidence-interval width is defined as

$$\overline{W} = \frac{1}{M} \sum_{m=1}^{M} (U_m - L_m),$$

where L_m and U_m are the lower and upper endpoints of CI_m, respectively.

8.2. Monte Carlo Results

The resulting Monte Carlo performance under the baseline transition matrix is summarized in Table 2. Additionally, Figure 4 shows the root mean square error (RMSE) of the estimated disease-network reliability for different sample sizes.

Table 2. Monte Carlo performance of the estimated disease-network reliability under the baseline transition matrix.

n	True $\mathcal{R}_H$	Mean $\widehat{\mathcal{R}}_H$	Bias	RMSE	Coverage	Average CI Width
100	0.7483	0.7427	−0.0056	0.0465	0.9333	0.1683
250	0.7483	0.7476	−0.0007	0.0274	0.9733	0.1075
500	0.7483	0.7489	+0.0006	0.0187	0.9500	0.0757
1000	0.7483	0.7483	−0.0000	0.0143	0.9533	0.0535
2000	0.7483	0.7477	−0.0006	0.0098	0.9467	0.0379

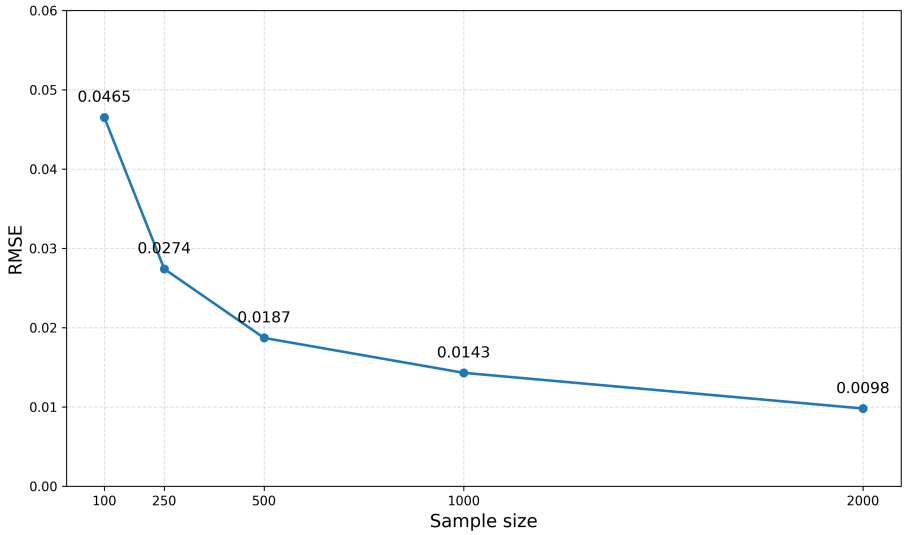


Figure 4. RMSE of the estimated disease-network reliability as a function of sample size.

The results show that the estimator becomes increasingly accurate as the number of observed patient trajectories increases. The absolute bias is small across all considered sample sizes and becomes negligible for $n \geq 500$. More importantly, the RMSE decreases consistently with sample size, from

$$0.0465$$

at $n = 100$ to

$$0.0098$$

at $n = 2000$. Thus, the simulation provides numerical evidence of the finite-sample stability of the proposed reliability estimator. The empirical coverage probabilities are close to the nominal 95% level across the considered sample sizes, ranging from 0.9333 to 0.9733. The average confidence-interval width decreases from 0.1683 at $n = 100$ to 0.0379 at $n = 2000$, indicating increasingly precise uncertainty quantification as the sample size increases.

8.3. Bootstrap Illustration

To illustrate the uncertainty quantification procedure, one simulated dataset containing $n = 1000$ patients is considered. Using $B = 2000$ patient-level bootstrap replications, the estimated reliability is

$$\widehat{\mathcal{R}}_H = 0.772,$$

with the corresponding percentile bootstrap confidence interval

$$\boxed{CI_{95\%} = (0.745, 0.798).}$$

The true baseline reliability,

$$\mathcal{R}_H^{\text{true}} = 0.74828,$$

lies within this interval.

This example illustrates the patient-level percentile bootstrap procedure. The empirical confidence-interval coverage and average interval width are evaluated across the $M = 300$ Monte Carlo replications and the five sample sizes reported in Table 2.

8.4. Constrained Sensitivity Results

The constrained sensitivity analysis is applied to the same baseline transition matrix. For each admissible transition, a row-preserving perturbation is applied as described in Section 6, and the corresponding elasticity

$$E_{ij} = \frac{p_{ij}}{\mathcal{R}_H} S_{ij}$$

is calculated. The resulting benchmark elasticity ranking is presented in Table 3.

Table 3. Constrained elasticity ranking of disease-state transitions.

Rank	Transition	Elasticity
1	$L \to T$	+0.2587
2	$T \to R$	+0.2115
3	$M \to R$	+0.1058
4	$M \to T$	+0.0259
5	$L \to M$	+0.0016
6	$T \to M$	−0.0393
7	$T \to D$	−0.0559
8	$M \to D$	−0.1053
9	$L \to D$	−0.1307

As a numerical stability check, the elasticity calculations were repeated using $\delta = 0.001$ and $\delta = 0.01$, in addition to the baseline value $\delta = 0.005$. The resulting transition ranking was unchanged across these three perturbation sizes, with only negligible differences in the reported elasticity values. This confirms that the identified transition ranking is not sensitive to the particular small perturbation size used in the finite-difference calculation. The largest positive elasticity is associated with the transition

$$L \to T,$$

indicating that this transition has the greatest positive local influence on the probability of reaching remission before death under the specified baseline network. In contrast, the most negative elasticity corresponds to

$$L \to D,$$

indicating that increasing the probability of direct transition from localized disease to death has the strongest negative local influence on the reliability measure.

These results demonstrate that the proposed framework provides information beyond the overall reliability value. In particular, it identifies individual transitions that are statistically important for the reliability of the disease progression network. Figure 5 presents the constrained elasticity values for the admissible disease-state transitions, highlighting the transitions with the strongest positive and negative effects on disease-network reliability.

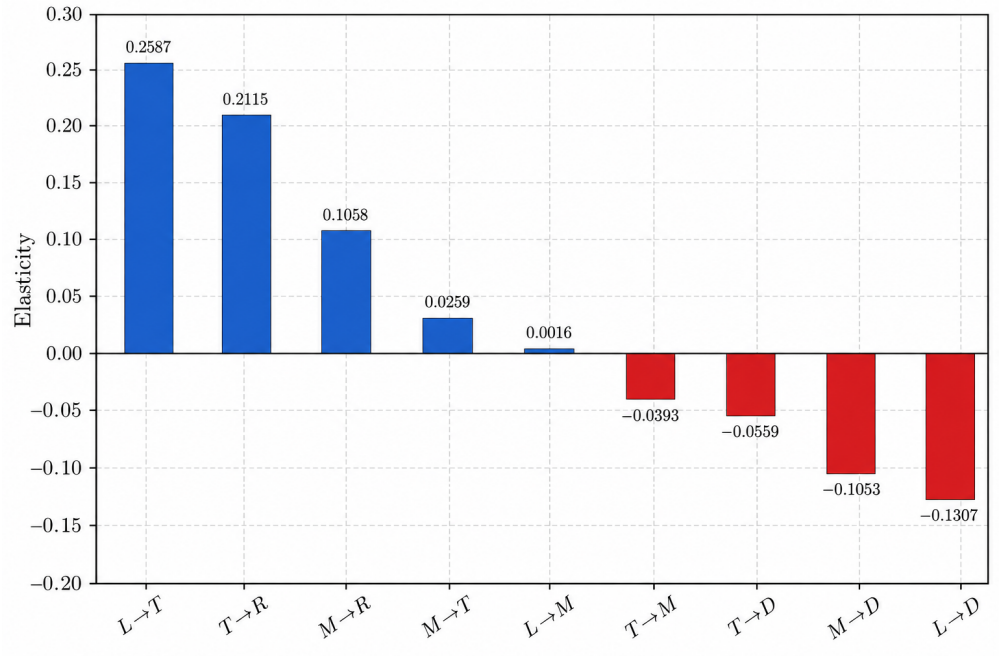


Figure 5. Transition elasticity heatmap for disease-network reliability.

9. Breast Cancer Application: Empirical Illustration

The proposed framework is illustrated using a longitudinal breast-cancer dataset containing records for $N = 169$ patients. The purpose of this application is to demonstrate how observable longitudinal patient records can be organized within the proposed transition-based statistical framework. Because the available data do not provide direct and independently verifiable observations for all seven theoretical states, the complete seven-state transition matrix and the corresponding reliability functional are not estimated from these data. Instead, the empirical analysis is restricted to clinical events that can be directly identified from the available records.

The available database contains demographic, pathological, treatment, surgical, recurrence, survival, and follow-up information. In particular, recorded dates include biopsy date, first-treatment date, surgery date, recurrence date, death date, and last-seen date. Thus, the database provides a natural longitudinal structure for evaluating the statistical ingredients of the proposed framework. Figure 6 illustrates the progression of breast cancer and its representation within the proposed statistical framework.

The empirical analysis is deliberately restricted to variables and events that are directly observable in the available records. States for which an unambiguous statistical

classification cannot be established are not inferred. This distinction is important because the theoretical state space

$$V = \{H, E, L, T, R, M, D\}$$

is a methodological representation, whereas an empirical state space must be supported by the actual information recorded for each patient.

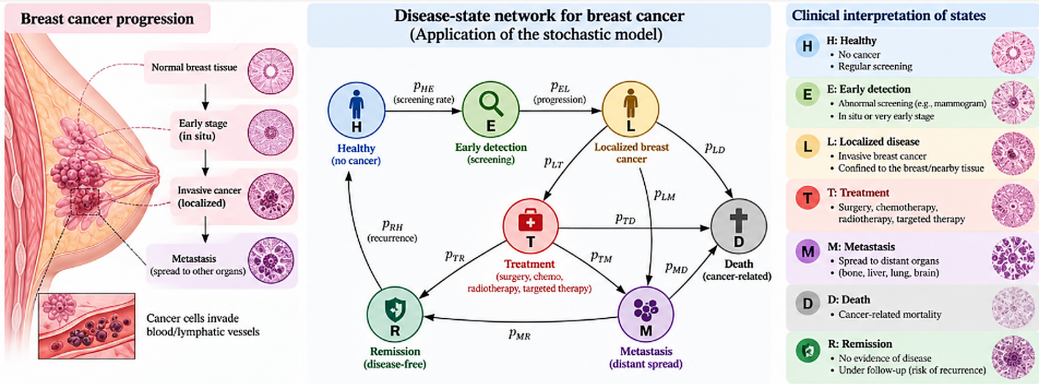


Figure 6. Breast-cancer disease progression and its representation within the proposed statistical framework.

Observed Longitudinal Structure

For patient k, let

$$\mathcal{Y}_k = (Y_{k0}, Y_{k1}, \ldots, Y_{km_k})$$

denote the ordered sequence of clinically recorded events, where m_k denotes the number of observed transitions between successive recorded events.

In contrast to the theoretical state sequence X_t used in Sections 2–6, the empirical event sequence $\mathcal{Y}_k$ is constructed only from variables that are directly recorded in the database. For the present dataset, the principal observed events are diagnosis/biopsy, first treatment, surgery, recurrence, and death, together with administrative follow-up.

Accordingly, the empirical analysis distinguishes between the theoretical state space and the observable event space:

$$\mathcal{O} = \{\mathrm{B}, \mathrm{T}, \mathrm{S}, \mathrm{Rec}, \mathrm{D}\},$$

where B denotes biopsy/diagnosis, T treatment, S surgery, Rec recurrence, and D death. This observable event representation is used for the empirical illustration of the observable component of the proposed framework. It does not replace the seven-state disease progression model defined earlier. earlier.

Figure 7 summarizes the empirically observed progression of patients through the recorded clinical events. The network shows a predominantly sequential pattern from biopsy/diagnosis to treatment and surgery, followed by recurrence for a subset of patients and death for a smaller subset. The transition from diagnosis to treatment and from treatment to surgery is observed for the majority of patients, whereas recurrence and death occur less frequently. The network therefore provides a direct statistical representation of the observed longitudinal structure of the dataset. Importantly, this empirical event network is used to illustrate the observable component of the proposed framework and does not imply that the observed events constitute a complete representation of the seven-state theoretical disease progression model.

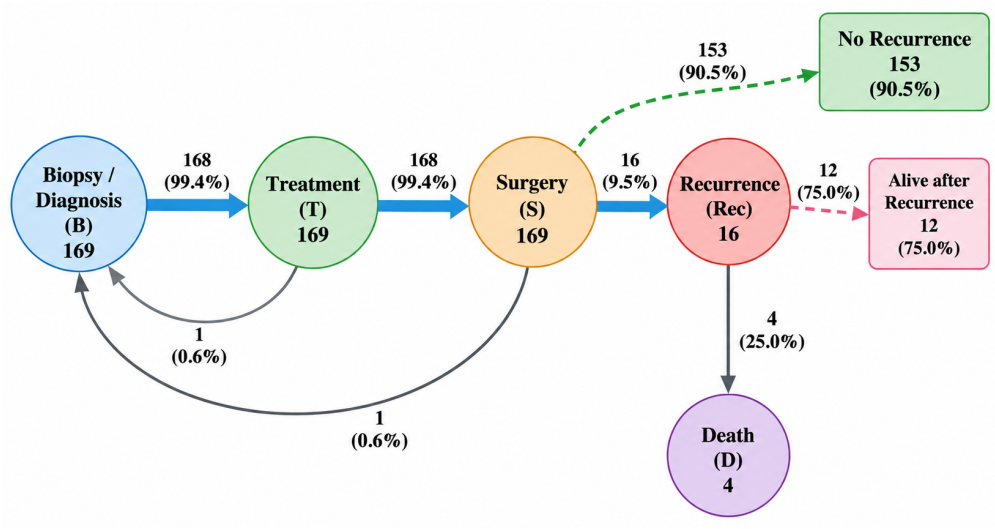


Figure 7. Empirically observed patient-event progression in the breast cancer dataset. Edge widths represent the number of observed transitions.

The available records show that all 169 patients have a biopsy date, a first-treatment date, a surgery date, and a last-seen date. Recurrence is recorded for 16 patients, while death is recorded for 4 patients. Therefore,

$$N = 169, \qquad N_{\mathrm{Rec}} = 16, \qquad N_{\mathrm{D}} = 4.$$

The corresponding empirical proportions are

$$\widehat{\pi}_{\mathrm{Rec}} = \frac{16}{169} = 0.0947,$$

and

$$\widehat{\pi}_{\mathrm{D}} = \frac{4}{169} = 0.0237.$$

Thus, approximately 9.47% of the observed patients experienced a recorded recurrence, whereas 2.37% experienced a recorded death during the available follow-up. Among the 16 patients with recorded recurrence, 4 subsequently had a recorded death. Hence the empirical conditional proportion is

$$\widehat{\pi}_{\mathrm{D}|\mathrm{Rec}} = \frac{4}{16} = 0.25.$$

Consequently,

$$\widehat{\pi}_{\mathrm{Rec}\setminus\mathrm{D}} = \frac{12}{16} = 0.75.$$

These quantities are descriptive empirical event probabilities. They are not interpreted as estimates of p_{LM}, p_{TR}, or any other element of the theoretical seven-state transition matrix unless the corresponding clinical-state mapping has been independently established.

Empirical Transition Counts

The statistical estimation procedure developed in Section 4 is based on transition counts. For a fully observed patient-level state sequence, define

$$n_{ij} = \sum_{k=1}^{N} \sum_{t=0}^{T_k - 1} I(X_{kt} = i, X_{k,t+1} = j),$$

where $I(\cdot)$ is the indicator function.

For the observable event sequence, the analogous count is

$$n_{ab}^{(\mathcal{O})} = \sum_{k=1}^{N} \sum_{t=0}^{m_k-1} I(Y_{kt} = a, Y_{k,t+1} = b), \qquad a, b \in \mathcal{O}.$$

If

$$n_a^{(\mathcal{O})} = \sum_{b \in \mathcal{O}} n_{ab}^{(\mathcal{O})}$$

is positive, the corresponding empirical conditional probability is

$$\widehat{p}_{ab}^{(\mathcal{O})} = \frac{n_{ab}^{(\mathcal{O})}}{n_a^{(\mathcal{O})}}.$$

This is the same maximum-likelihood principle used for the theoretical transition matrix. Indeed, if the observations associated with state i are independent conditional on the current state, the row likelihood is

$$L_i(\mathbf{p}_i) = \prod_{j \in V} p_{ij}^{n_{ij}},$$

subject to

$$p_{ij} \geq 0, \qquad \sum_{j \in V} p_{ij} = 1.$$

The resulting maximum-likelihood estimator is

$$\boxed{\widehat{p}_{ij} = \frac{n_{ij}}{\sum_{j'} n_{ij'}}}.$$

Hence, the proposed transition estimator is directly interpretable as a multinomial maximum-likelihood estimator for each row of the transition matrix. For the present breast-cancer data, however, the complete seven-state transition counts n_{ij} cannot be constructed without imposing additional assumptions about unrecorded states. In particular, the available records do not provide an independently verified classification of all patients into the theoretical states H, E, L, R, and M at successive observation occasions. Therefore, a complete numerical estimate of the seven-state matrix $\widehat{P}$ is not reported from these data.

9.1. Observed Event-Time Structure

Although the complete state-transition matrix is not identifiable, the recorded dates provide direct information about the temporal ordering of major observed events. For patient k, define the observed time intervals

$$\Delta_k^{(B,T)} = t_{k,T} - t_{k,B},$$

$$\Delta_k^{(T,S)} = t_{k,S} - t_{k,T},$$

and

$$\Delta_k^{(B,S)} = t_{k,S} - t_{k,B}.$$

For patients with recurrence,

$$\Delta_k^{(B,\mathrm{Rec})} = t_{k,\mathrm{Rec}} - t_{k,B},$$

and for patients with recorded death,

$$\Delta_k^{(B,D)} = t_{k,D} - t_{k,B}.$$

The empirical summaries are presented in Table 4.

Table 4. Observed longitudinal time intervals in the breast-cancer dataset. The negative value of −113 days for the biopsy-to-first-treatment interval corresponds to one anomalous record in which the recorded treatment date preceded the biopsy date. This record was retained as a data-quality anomaly and was not interpreted as a valid negative treatment delay.

Interval	*n*	Median	Mean	Range (Days)
Biopsy → first treatment	169	32.0	35.11	−113–141
First treatment → surgery	169	181.0	179.48	74–503
Biopsy → surgery	169	213.0	214.59	121–578
Surgery → recurrence	16	684.0	769.06	34–1694
Surgery → death	4	1252.0	1357.75	836–2091

The median interval from biopsy to first treatment is 32 days, whereas the median interval from first treatment to surgery is 181 days. The median biopsy-to-surgery interval is therefore 213 days.

For patients with recorded recurrence, the median time from biopsy to recurrence is 684 days. Among the four patients with recorded death, the median biopsy-to-death interval is 1252 days. These observed intervals provide an empirical temporal structure for the patient trajectories and demonstrate that the database contains repeated longitudinal information rather than a single cross-sectional measurement.

Figure 8 shows the distributions of the main clinically observed time intervals in the breast cancer dataset. The median time from biopsy/diagnosis to first treatment was 32 days, whereas the median time from first treatment to surgery was 181 days. The median interval from biopsy/diagnosis to surgery was 213 days, indicating that the treatment and surgical stages account for a substantial portion of the observed progression time. Among patients with recorded recurrence, the median time from diagnosis to recurrence was 684 days, with noticeably greater variability than the earlier treatment-related intervals. The wider spread observed for the recurrence interval reflects substantial heterogeneity in the timing of disease recurrence across patients. These empirical distributions provide a statistical description of the observed longitudinal follow-up and support the use of transition-based analysis for the subsequent reliability framework.

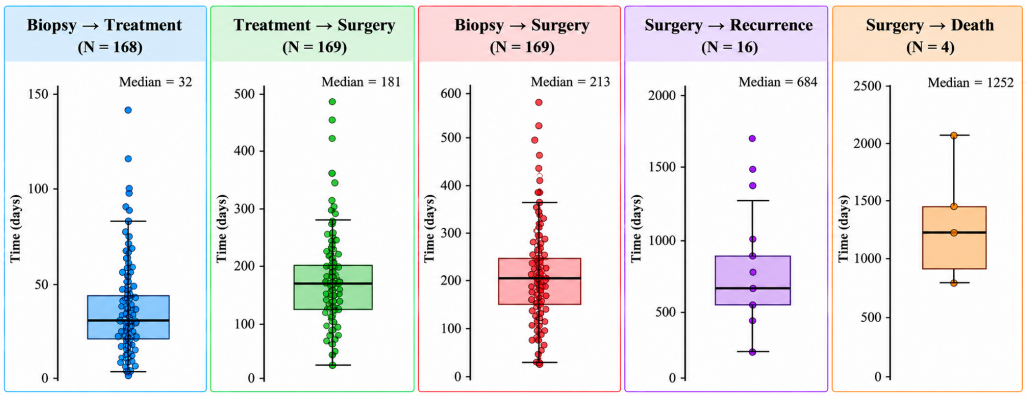


Figure 8. Distribution of clinically relevant observed time intervals in the breast cancer dataset. Box-plots summarize the observed time intervals between diagnosis, treatment, surgery, and recurrence.

Empirical Outcome Structure

The observed clinical outcomes can be summarized by the following empirical count decomposition:

$$N = N_{\text{neither}} + N_{\text{Rec}}$$

with

$$153 + 16 = 169.$$

The recurrence group can further be decomposed as

$$N_{\text{Rec}} = N_{\text{Rec},D} + N_{\text{Rec},\overline{D}},$$

where

$$4 + 12 = 16.$$

The resulting outcome is given in Table 5.

Table 5. Observed recurrence and death outcomes.

Outcome	Number	Percentage
No recorded recurrence	153	90.53%
Recorded recurrence	16	9.47%
Recorded death	4	2.37%
Death among recurrence cases	4/16	25.00%
Recurrence without recorded death	12/16	75.00%

An important feature of the observed data is that all four recorded deaths occur among patients with a previously recorded recurrence. Thus, within this dataset,

$$\{\text{Death}\} \subset \{\text{Recurrence}\}.$$

This empirical ordering is consistent with the interpretation of the records as longitudinal trajectories and illustrates the usefulness of representing clinical information as an ordered transition structure.

It should nevertheless be emphasized that recurrence cannot automatically be identified with the theoretical metastasis state M, and absence of a recurrence record cannot automatically be identified with remission R. Such mappings would require a validated clinical variable dictionary and would introduce assumptions that are not supported by the available data.

9.2. Application of the Statistical Framework

The reliability functional, patient-level bootstrap procedure, and row-preserving transition sensitivity analysis developed in the preceding methodological sections provide the statistical tools for analyzing the disease-progression network. In a completely observed seven-state dataset, the estimated reliability is obtained by applying the previously defined functional to the estimated transition matrix, Equation (4).

Sampling uncertainty is then assessed using the patient-level bootstrap, and transition importance is evaluated using the row-preserving sensitivity procedure described in Section 6. For the present breast-cancer dataset, these procedures are not used to produce a numerical seven-state reliability estimate because the required clinical state classification is not fully identifiable. The purpose of the empirical application is instead to demonstrate the observable longitudinal information, assess its temporal consistency, and identify the data requirements needed for a complete implementation of the proposed reliability framework.

9.3. Empirical Interpretation and Illustration

The breast-cancer records provide three important forms of empirical illustration for the proposed framework. First, the data contain complete longitudinal data information for the main recorded clinical events. This permits patient-level trajectories to be ordered temporally and demonstrates the practical basis for transition-based statistical analysis. Second, the observed recurrence and death events illustrate competing outcome information. In particular,

$$\widehat{\pi}_{\mathrm{Rec}} = 0.0947$$

and

$$\widehat{\pi}_{\mathrm{D|Rec}} = 0.25$$

show how event probabilities can be obtained directly from patient-level records without introducing a mechanistic disease model. Third, the empirical analysis demonstrates an important statistical principle of the proposed methodology: **state definitions must be identifiable before transition probabilities and network reliability can be estimated. The theoretical reliability, Equation (1), requires explicit identification of the transient states and the remission/death boundary states. The available dataset begins with patients already recorded at breast-cancer diagnosis and therefore does not directly observe the theoretical healthy state H or the early-detection state E. Similarly, the variables available in the current file do not provide a sufficiently verified basis for assigning every patient to the theoretical states R and M.

Consequently, replacing the unavailable states by assumptions would create artificial transition probabilities and would undermine the statistical validity of the reliability estimator. The correct empirical interpretation is therefore

$$\boxed{\text{observed patient records} \rightarrow \text{identifiable events} \rightarrow \text{empirical transition information}}$$

while the complete theoretical framework remains

$$\boxed{\text{patient state trajectories} \rightarrow \widehat{P} \rightarrow \widehat{\mathcal{R}}_H \rightarrow CI_{95\%} \rightarrow \text{transition importance.}}$$

The controlled Monte Carlo study in Section 7 and the breast-cancer illustration serve complementary purposes: the simulation evaluates the statistical behavior of the reliability estimator under a known transition network, whereas the real-data analysis demonstrates the longitudinal information available from patient records and identifies the data requirements for a complete reliability analysis.

A basic temporal consistency check identified one record with an anomalous date ordering involving the chemotherapy-related date variable. In that record, the recorded last-chemotherapy date precedes the biopsy date. Rather than silently modifying or deleting the observation, the anomaly is retained and flagged as a data-quality issue. This is consistent with the statistical philosophy of the proposed framework: transition estimation should be based on explicitly defined and validated observations.

Importantly, the anomaly does not alter the principal biopsy-to-treatment, treatment-to-surgery, biopsy-to-surgery, recurrence, and death intervals reported above because those calculations use the corresponding event dates directly. This check also illustrates why empirical transition analysis requires careful verification of event ordering before constructing n_{ij} and $\widehat{P}$.

10. Discussion

The proposed framework provides an integrated statistical approach for representing disease progression as a patient-level directed transition network and for transforming the estimated transition structure into an outcome-oriented reliability measure. The framework combines four main statistical components:

transition estimation → network reliability → bootstrap uncertainty → constrained sensitivity.

The central quantity,

$$\mathcal{R}_H = P_H(\tau_R < \tau_D),$$

has a direct probabilistic interpretation: it represents the probability that a patient starting from the initial state reaches the target remission state before the adverse absorbing state of death. Unlike an individual transition probability, $\mathcal{R}_H$ integrates all admissible pathways through the transient network. The matrix representation, Equation (1), therefore provides a compact summary of the global behavior of the estimated disease-transition structure. The proposed framework should not be interpreted as claiming that multistate Markov modeling itself is novel. Markov and multistate models are well-established statistical tools for disease progression [3,4], and recent methodological developments continue to address model assessment, uncertainty, and complex multistate processes [5]. The methodological contribution of the present study is instead the explicit integration of transition estimation, first-hit network reliability, bootstrap uncertainty quantification, and row-constrained transition sensitivity within a single statistical framework. A central statistical feature is that the reliability is a nonlinear functional of the transition probabilities. Consequently, sampling variability in the estimated transition matrix propagates to the reliability estimate. The differential identity

$$d\mathcal{R}_H = \mathbf{e}_H^\top (\mathbf{I} - \mathbf{Q})^{-1}[(dQ)\mathbf{r} + d\mathbf{b}]$$

makes this propagation explicit. This also provides the mathematical basis for the transition-level sensitivity analysis and explains why uncertainty should not be assessed solely at the level of individual transition probabilities.

The bootstrap procedure complements this analytical representation by resampling complete patient trajectories rather than individual transitions. This preserves the dependence structure within each patient's trajectory and allows the complete reliability functional to be recalculated for each bootstrap sample. Thus, the uncertainty analysis follows the same statistical pathway as the estimator itself:

$$\widehat{P}^{*(b)} \longrightarrow \widehat{Q}^{*(b)} \longrightarrow \widehat{\mathcal{R}}_H^{*(b)}.$$

The resulting empirical distribution provides a direct basis for estimating the sampling variability and constructing a percentile confidence interval [8,9,14]. The constrained sensitivity analysis is also important from a statistical perspective. The elements of a transition-matrix row cannot be varied independently because

$$\sum_j p_{ij} = 1.$$

Therefore, an unconstrained perturbation of a single transition probability generally produces an invalid probability vector. The proposed row-preserving perturbation instead moves the probability vector along the simplex

$$\Delta_i = \left\{ \mathbf{p}_i : p_{ij} \geq 0, \sum_j p_{ij} = 1 \right\}.$$

This provides a statistically valid basis for comparing the local influence of different transitions on the global reliability measure. The Monte Carlo results provide numerical evidence for the finite-sample behavior of the proposed estimator. Under the specified baseline transition matrix, the true reliability is

$$\mathcal{R}_H^{\text{true}} \approx 0.7483.$$

The simulation results show a systematic reduction in RMSE as the number of patient trajectories increases. Specifically, the RMSE decreases from approximately 0.0465 for $n = 100$ to 0.0098 for $n = 2000$. This behavior is consistent with increasing statistical precision as more patient trajectories become available.

The sensitivity results provide additional information beyond the overall reliability. Under the baseline network, the largest positive elasticity is associated with

$$L \to T,$$

with elasticity approximately

$$E_{LT} = 0.2587.$$

The transition

$$T \to R$$

has the second largest positive elasticity,

$$E_{TR} = 0.2115.$$

In contrast, the most negative elasticity is associated with

$$L \to D,$$

with

$$E_{LD} = -0.1307.$$

These results illustrate that the statistical importance of a transition is determined not only by its probability but also by its location within the network and by the alternative pathways available from that state.

The real breast-cancer application provides an important complementary perspective. The dataset contains 169 patient records with longitudinal information on diagnosis, treatment, surgery, recurrence, death, and follow-up. Sixteen patients had a recorded recurrence and four had a recorded death. The observed recurrence proportion is therefore

$$\frac{16}{169} = 0.0947,$$

while the recorded death proportion is

$$\frac{4}{169} = 0.0237.$$

Among patients with recurrence, the observed proportion with subsequent recorded death is

$$\frac{4}{16} = 0.25.$$

These empirical quantities demonstrate that the available data contain the longitudinal event information required for a transition-based statistical analysis. The median time from biopsy to first treatment is 32 days, the median time from first treatment to surgery is 181 days, and the median time from biopsy to surgery is 213 days. For patients with recorded recurrence, the median biopsy-to-recurrence time is 684 days.

An important methodological finding from the empirical application is that the complete seven-state transition matrix cannot be identified from the available variables without introducing additional assumptions. In particular, the database begins with patients already observed at the diagnosis stage and therefore does not directly provide longitudinal observations of the theoretical states H and E. Furthermore, the available variables do not provide sufficient validated information for unambiguously classifying every patient into the theoretical remission state R or distant-metastasis state M.

This limitation is statistically important. Estimating

$$\widehat{p}_{ij} = \frac{n_{ij}}{\sum_j n_{ij}}$$

requires an identifiable state sequence. Similarly, Equation (4) requires identifiable estimates of all transition probabilities entering Q and $\mathbf{b}$. Therefore, assigning unverified clinical variables to R or M merely to obtain a numerical reliability estimate would introduce model-based information that is not contained in the observed data.

For this reason, the empirical application is interpreted as an illustration of the data-to-transition component of the framework rather than as a claim of a fully identified seven-state reliability estimate.

The distinction between simulation and empirical analysis is therefore essential. In the Monte Carlo experiment, the complete transition matrix is known and the statistical properties of

$$\widehat{\mathcal{R}}_H$$

can be evaluated directly through bias and RMSE. In the real-data analysis, the observed longitudinal records establish the feasibility of constructing patient-level trajectories and transition information, while the identifiability assessment determines which components of the theoretical model can legitimately be estimated.

The current empirical dataset reaches the first stages of this pipeline directly and demonstrates the type of longitudinal information required for the subsequent stages. A complete seven-state empirical reliability analysis would require a validated state-classification scheme that maps the recorded clinical variables to the theoretical states without ambiguity.

Several limitations should therefore be acknowledged. First, the Markov assumption is a modeling assumption and may be affected by patient heterogeneity, unequal observation intervals, state misclassification, or dependence on a longer clinical history [3,10]. Second, the current empirical dataset is relatively small for estimating rare transitions such as death. Third, administrative censoring and incomplete observation of intermediate states can prevent direct construction of the complete transition matrix. Fourth, the present framework uses a discrete-time representation and therefore requires a common observation scale when successive observations are used as Markov transitions.

These limitations do not invalidate the proposed framework; rather, they define the conditions under which its empirical implementation is statistically justified. Future studies with larger longitudinal cohorts and validated state definitions can estimate the complete transition matrix, apply the reliability functional directly to observed trajectories, and quantify uncertainty and transition importance entirely from empirical data.

11. Conclusions

This study developed a unified statistical reliability framework for disease progression networks based on discrete-time Markov transitions. The framework combines transition estimation, first-passage reliability, bootstrap uncertainty quantification, and probability-constrained sensitivity analysis. The Monte Carlo results demonstrated increasing estimation stability as the sample size increased, with RMSE decreasing from 0.0465 at $n = 100$ to 0.0098 at $n = 2000$ for a baseline reliability of approximately 0.7483. The sensitivity analysis identified treatment- and remission-related transitions as important positive contributors to reliability, while transitions toward death had negative effects. Application to 169 real breast cancer patients identified 16 recurrence events and four deaths and demonstrated the practical value of the proposed statistical approach for analyzing longitudinal patient-event patterns. Since the available clinical variables do not uniquely identify all seven theoretical states, the empirical analysis was restricted to observable events without imposing unsupported state assignments.

Author Contributions: Conceptualization, K.A.A.; Methodology, T.M.A.; Software, N.A.A.; Validation, N.A.A. and T.M.A.; Formal analysis, K.A.A.; Investigation, M.F.A.-H.; Resources, M.M.A.-B.; Writing—original draft preparation, M.A.S.; Writing—review and editing, M.A.S.; Supervision, M.A.S. All authors have read and agreed to the published version of the manuscript.

Funding: This research was funded by Qassim University (QU-APC-2026).

Institutional Review Board Statement: The institutional review board (IRB) approval was waived because this study is a secondary analysis of a publicly available, fully anonymized dataset ("Clinical dataset for HER2-positive breast cancer analysis", https://doi.org/10.5281/zenodo.15231828 accessed on 19 October 2026), involving no identifiable private information. The original study was approved by the Ethical Review Board of the Medical University of Vienna (Approval No. 1723/2019).

Informed Consent Statement: Informed consent was waived for this secondary analysis because the dataset is publicly available and fully anonymized.

Data Availability Statement: The breast cancer dataset analyzed in this study is publicly available through Zenodo at https://doi.org/10.5281/zenodo.15231828. The dataset is an anonymized longitudinal clinical dataset of patients with HER2-positive breast cancer. It contains information related to diagnosis, pathology, treatment, surgery, recurrence, survival, and follow-up. The present study used the dataset solely for statistical analysis of observable patient-level events.

Acknowledgments: The researchers would like to thank the Deanship of Graduate Studies and Scientific Research at Qassim University for financial support (QU-APC-2026).

Conflicts of Interest: The authors declare no conflicts of interest.

References

1. Elbaz, I.M.; El-Metwally, H.; Sohaly, M.A. Viral kinetics, stability and sensitivity analysis of the within-host COVID-19 model. *Sci. Rep.* **2023**, *13*, 11675. [CrossRef] [PubMed]
2. Tanchev, D.; Marazov, A.; Balieva, G. Bayesian Inference for Graph-Based Markov Chain Model of African Swine Fever Transmission. *Mach. Learn. Knowl. Extr.* **2026**, *8*, 311. [CrossRef]
3. Jackson, C.H.; Sharples, L.D.; Thompson, S.G.; Duffy, S.W.; Couto, E. Multistate Markov models for disease progression with classification error. *Statistician* **2003**, *52*, 193–209. [CrossRef]
4. Meira-Machado, L.; de Uña-Alvarez, J.; Cadarso-Suárez, C.; Andersen, P.K. Multi-state models for the analysis of time-to-event data. *Stat. Methods Med. Res.* **2009**, *18*, 195–222. [CrossRef] [PubMed]
5. Gorfine, M.; Cook, R.J.; Andersen, P.K.; Therneau, T.M.; Joly, P.; Putter, H.; Pohar Perme, M.; Abrahamowicz, M. An overview and recent developments in the analysis of multistate processes. *Stat. Med.* **2026**, *45*, e70493. [CrossRef] [PubMed]
6. Zingoni, Z.M.; Chirwa, T.F.; Todd, J.; Musenge, E. A review of multistate modelling approaches in monitoring disease progression: Bayesian estimation using the Kolmogorov-Chapman forward equations. *Stat. Methods Med. Res.* **2021**, *30*, 1373–1392. [CrossRef] [PubMed]

7. Akwiwu, E.U.; Coupé, V.M.H.; Berkhof, J.; Klausch, T. A Comparison of Methods for Modeling Multistate Cancer Progression Using Screening Data with Censoring after Intervention. *Med. Decis. Mak.* **2026**, *46*, 575–590. [CrossRef] [PubMed]
8. Craig, B.A.; Sendi, P.P. Estimation of the transition matrix of a discrete-time Markov chain. *Health Econ.* **2002**, *11*, 33–42. [CrossRef] [PubMed]
9. Welton, N.J.; Ades, A.E. Estimation of Markov chain transition probabilities and rates from fully and partially observed data: Uncertainty propagation, evidence synthesis, and model calibration. *Med. Decis. Mak.* **2005**, *25*, 633–645. [CrossRef] [PubMed]
10. Titman, A.C.; Sharples, L.D. Model diagnostics for multi-state models. *Stat. Methods Med. Res.* **2010**, *19*, 621–651. [CrossRef] [PubMed]
11. Natvig, B. Multistate system reliability. In *Wiley Encyclopedia of Operations Research and Management Science*; Cochran, J.J., Cox, L.A., Jr., Keskinocak, P., Kharoufeh, J.P., Smith, J.C., Eds.; Wiley: Hoboken, NJ, USA, 2011. [CrossRef]
12. Wei, Y.; Cheng, Y.; Liao, H.; Elsayed, E.A. Resilience modeling for an engineered network with multimodal performance under multiple recurrent hazards. *Reliab. Eng. Syst. Saf.* **2026**, *266*, 111640. [CrossRef]
13. Kemeny, J.G.; Snell, J.L.; Knapp, A.W. Introduction to potential theory. In *Denumerable Markov Chains: With a Chapter of Markov Random Fields by David Griffeath*; Springer: New York, NY, USA, 1976; pp. 166–190.
14. Efron, B.; Tibshirani, R.J. *An Introduction to the Bootstrap*; Chapman & Hall: New York, NY, USA, 1993.

Disclaimer/Publisher's Note: The statements, opinions and data contained in all publications are solely those of the individual author(s) and contributor(s) and not of MDPI and/or the editor(s). MDPI and/or the editor(s) disclaim responsibility for any injury to people or property resulting from any ideas, methods, instructions or products referred to in the content.